

Non-Förster distance and orientation dependence of energy transfer and applications of fluorescence resonance energy transfer to polymers and nanoparticles: How accurate is the spectroscopic ruler with $1/R^6$ rule?

Harjinder Singh^{1,2} and Biman Bagchi^{1,*}

¹Solid State and Structural Chemistry Unit, Indian Institute of Science, Bangalore 560 012, India

²On leave from Department of Chemistry, Panjab University, Chandigarh 160 014, India

Fluorescence resonance energy transfer (FRET) is a popular tool to study equilibrium and dynamical properties of polymers and biopolymers in condensed phases and is now being widely used in conjunction with single molecule spectroscopy. The rate of FRET is usually assumed to be given by the Förster expression:

$$k_F = k_{\text{rad}} \left(\frac{R_F}{R} \right)^6,$$

where k_{rad} is the radiative rate (typically less than 10^9 s^{-1}) and R_F is the well-known Förster radius which is given by the spectral overlap between the fluorescence spectrum of the donor and the absorption spectrum of the acceptor. We first present a critical analysis of the derivation of the above expression and argue why this expression can be of limited validity in many cases. We demonstrate this by explicitly considering a donor–

acceptor system, polyfluorene (PF₆)-tetraphenylporphyrin (TPP), where their sizes are comparable to the distance separating them. In such cases, one may expect much weaker distance (as $1/R^2$ or even weaker) dependence. Another limitation is that optically dark states can make significant contribution to the energy transfer rate – these contributions are neglected in the Förster expression. Yet another limitation is that Förster, being based on Fermi Golden Rule, neglects vibrational energy relaxation which can be a serious limitation when the rate is in the few picoseconds regime. We have also considered the case of energy transfer from a dye to a nanoparticle. Here we show that the distance dependence can be completely different from Förster and can give rise to $1/R^4$ distance dependence at large separations. We also discuss recent applications of FRET to study biopolymer conformational dynamics and an interesting breakdown of the famous Wilemski–Fixman theory.

Keywords: Conjugated polymers, Förster expression, FRET, nanoparticles, polymers dynamics, spectroscopic ruler.

THE usefulness of fluorescence resonance energy transfer (FRET) arises from the strong and simple distance dependence of the excitation energy transfer rate^{1,2}. The sensitivity of FRET to distance has led to this technique being regarded as a ‘spectroscopic ruler’³. The Förster expression is based on the Coulombic interaction between the donor and the acceptor, and a point dipole approximation of the interaction energy. The expression in its most common form is given by:

$$k_F = k_{\text{rad}} \left(\frac{R_F}{R} \right)^6. \quad (1)$$

In addition to applications in single molecule spectroscopy and biomolecular dynamics, such as protein folding, För-

ster energy transfer mechanism has been implicated and critically scrutinized in energy transfer in thin films of conjugated polymers. These systems are organic semiconductors with interesting opto-electronic properties. Host–guest systems comprised of polymer/polymer and polymer/dye blends offer colour tunability and can be used as colour emission in display systems⁴. Cerullo *et al.*⁵ have carried out femtosecond pump-probe experiments and observed ultra fast energy transfer in the picoseconds timescale⁵. Experiments by Barbara and coworkers⁶ have revealed evidence of an energy funnel in thin films of MEH–PPV, where the absorption spectrum is broad meaning many absorbers are present at different energies, while the emission spectrum is narrow and red shifted, suggesting the existence of a photochemical funnel. The existence of such a funnel would require efficient and fast excitation energy transfer. While a ‘particle in a box’ model predicts that the oscillator strength/radiative rate is proportional to the length of a polymer segment and thus can offer a qualitative understanding of energy migration to a funnel, a quantitative theory of these phenomena is yet to be developed.

*For correspondence. (e-mail: bbagchi@sscu.iisc.ernet.in)

Resonance energy transfer has also been widely used in the study of protein folding and dynamics of DNA and RNA⁷⁻⁹. Other studies include monitoring of competing Förster-type energy transfer pathways in single bichromophoric molecules¹⁰ and development of intelligent sensor for metal ions based on FRET^{11,12}.

In the present article we shall discuss distance dependence of resonance energy transfer via Coulomb mechanism. It was found that the Förster expression of $1/R^6$ dependence breaks down at short distances. We shall also discuss the use of FRET in polymer dynamics and protein folding.

Theoretical formulation

A schematic description of the excitation energy transfer (EET) from a donor to an acceptor is shown in Figure 1. EET is seen as an energetically downhill transformation from an initial state, $|\{D^e A_g\}\rangle$, to a final state, $|\{D_g A^e\}\rangle$, where $D_g(A_g)$ and $D^e(A^e)$ denote the ground and excited states of the donor (acceptor) molecules (or molecular aggregates) respectively. In what follows, we will refer to the donor and acceptor as if these are single molecules, though in reality they may be aggregate complexes. The vibrational manifold shown on the left in Figure 1 is associated with the initial configuration $\{D^e A_g\}$ and those shown on the right are the corresponding states for the final configuration $\{D_g A^e\}$. In realistic situations with the EET taking place in a subpicosecond time scale, the vibrational manifold does not get the opportunity to relax to the thermal equilibrium distribution. In other words, even for a single initial and a single final electronic configuration, the EET is a set of processes from a collective initial set of vibrational energy states to another collective final set of vibrational energy states. However, influence of the non-equilibrium vibrational distribution is only poorly understood at this stage and is an active area of research¹³. A better understanding in this area will be useful in many problems

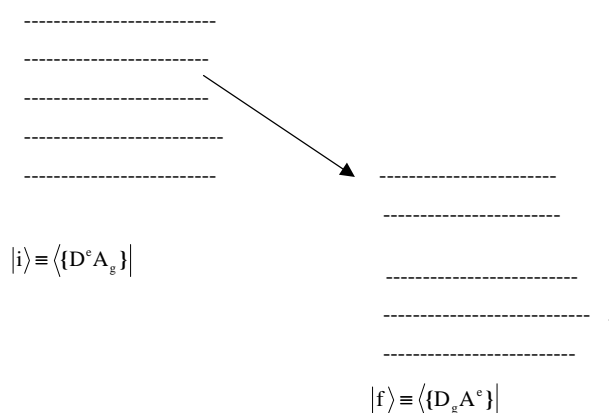


Figure 1. Schematic diagram of excitation energy transfer from a donor to an acceptor. Electronic states for the excited state of donor and ground state of acceptor are shown together with the corresponding vibrational manifolds.

of contemporary interest, e.g. that of the photosynthetic light harvesting systems and biomimetic photovoltaic devices^{14,15}.

The total Hamiltonian, \hat{H} , for the problem is divided into a noninteracting, \hat{H}_0 , and an interacting, \hat{H}' , parts.

$$\hat{H} = \hat{H}_0 + \hat{H}'. \quad (2)$$

Typically,

$$\hat{H}_0 = \hat{H}_{el} + \hat{H}_{vib} + \hat{H}_{el-vib}, \quad (3)$$

where \hat{H}_{el} , \hat{H}_{vib} and \hat{H}_{el-vib} are the purely electronic, purely vibrational (including reorganization energy for displaced oscillators) and the electronic–vibrational coupling parts of the individual molecules respectively. The part describing the interaction \hat{H}' can be fairly complex, since it involves the details of chemistry of the donor and the acceptor and also the medium.

An exact description of dynamics of the system is given in terms of the time evolution of the density operator, $\mathbf{r}(t)$, for the system as follows¹⁶:

$$\frac{d}{dt} \mathbf{r}(t) = -i\hat{L}\mathbf{r}(t) = -i(\hat{L}_0 + \hat{L}')\mathbf{r}(t). \quad (4)$$

Here \hat{L} is the Liouville operator with components \hat{L}_0 and \hat{L}' , such that

$$\hat{L}_0 \mathbf{r} = \frac{1}{\hbar} [\hat{H}_0, \mathbf{r}]; \quad \hat{L}' \mathbf{r} = \frac{1}{\hbar} [\hat{H}', \mathbf{r}]. \quad (5)$$

It is useful to extract the electronic part of the problem using a projection operator, \hat{P} ,

$$\hat{P}A \equiv \sum_j |j\rangle \langle j| Z_j^{eq} Tr_{\{v\}}(A_{jj}), \quad (6)$$

where $|j\rangle$ is a member of the set of electronic eigenstates $\{|D^e A_g\rangle, |D_g A^e\rangle\}$; $A_{jj} = \langle j|A|j\rangle$ and Tr is the trace operator operating over the vibrational coordinates in this case. The factor Z_j^{eq} is the equilibrium canonical partition function for the Hamiltonian \hat{H}_0 , thus explicitly introducing the assumption of an equilibrium model. A reduced equation of motion, the Nakajima–Zwanzig equation, is then derived for the projected part of the total density matrix,

$$\begin{aligned} \frac{d}{dt} \hat{P}\mathbf{r}(t) = & -i\hat{P}\hat{L}e^{-i\hat{Q}\hat{L}t} \hat{Q}\mathbf{r}(0) - i\hat{P}\hat{L}'\hat{P}\mathbf{r}(t) \\ & - \int_0^t dt_1 \hat{P}\hat{L}e^{i\hat{Q}\hat{L}(t-t_1)} \hat{Q}\hat{L}'\hat{P}\mathbf{r}(t_1). \end{aligned} \quad (7)$$

Assuming that the vibrational levels are initially in the canonical distribution, and expanding \hat{L} keeping terms of up to second order in \hat{H}' , one gets a much simpler equation,

$$\frac{d}{dt} \hat{P} \mathbf{r}(t) = - \int_0^t dt_1 \hat{P} \hat{L}' e^{i\hat{L}_0(t-t_1)} \hat{L}' \hat{P} \mathbf{r}(t_1). \quad (8)$$

Assuming that vibrational relaxation occurs prior to EET (thus reaching equilibrium), allowing for a timescale approximation between the projected and the complementary parts, a Markovian master equation is obtained for the population elements of the electronic density matrix,

$$\frac{d}{dt} \tilde{\mathbf{r}}_{jj}(t) = - \sum_{k \neq j} W_{kk, jj} \tilde{\mathbf{r}}_{jj}(t) + \sum_{k \neq j} W_{jj, kk} \tilde{\mathbf{r}}_{kk}(t), \quad (9)$$

where $\tilde{\mathbf{r}} \equiv \hat{P} \mathbf{r}$ and

$$W_{jj, kk} = 2 \text{Re} \int_0^\infty dt T r_{\{v\}}(e^{iH_{0k}t} H'_{kj} e^{-iH_{0j}t} H'_{jk} \mathbf{r}_k^{\text{eq}}). \quad (10)$$

The Coulomb coupling approximation

The operator \hat{H}' may be simplified such that it contains only the Coulombic coupling between the charge distributions of the donor and the acceptor.

$$\hat{H}' = H^{\text{Coul}}. \quad (11)$$

Rigorously, H^{Coul} may be defined as

$$H^{\text{Coul}} = V_{\text{DA}} |D^e A_g\rangle \langle D_g A^e| + \text{h.c.} \quad (12)$$

With this eq. (10) is transformed into

$$W_{jj, kk} = 2 |V_{\text{DA}}|^2 \text{Re} \int_0^\infty dt \mathbf{f}_{D^e A_g}^*(\mathbf{t}) A_{D_g A^e}(\mathbf{t}). \quad (13)$$

With energies measured relative to the corresponding ground states (Figure 2), $F_{D^e A_g}^*(\mathbf{t})$ and $A_{D_g A^e}(\mathbf{t})$ can be written as $F_D^*(\mathbf{t})$ and $A_A(\mathbf{t})$ respectively and using Fourier transforms $f(\mathbf{w}) = \int_{-\infty}^\infty dt e^{i\mathbf{w}t} f(t)$, eq. (13) is further modified as,

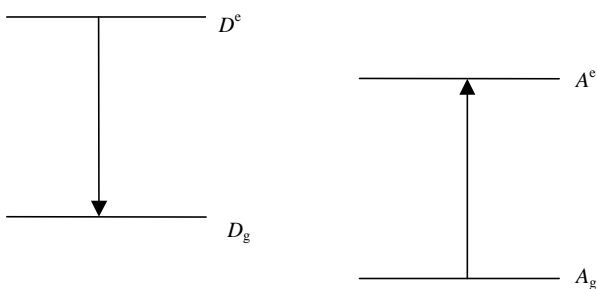


Figure 2. Separated donor and acceptor processes in a resonant energy transfer. A concerted de-excitation of the donor and absorption by the acceptor.

$$W_{jj, kk} = \frac{|V_{\text{DA}}|^2}{2p} \int_{-\infty}^\infty d\mathbf{w} \tilde{F}_D(\mathbf{w}) \tilde{A}_A(\mathbf{w}). \quad (14)$$

The quantities $\tilde{F}_D(\mathbf{w})$ and $\tilde{A}_A(\mathbf{w})$ are related to the line-shape functions for the emission spectrum of the donor and the absorption coefficient of the acceptor molecules, except for a few constants. In eq. (14) we have shown a fairly general derivation of Förster rate equation. It is valid as long as the interaction between the donor D and the acceptor A can be separated out.

This assumption ignores the fact that as quantum mechanical entities, the donor and acceptor molecules may have superposition of wave functions leading to complex effects. Such effects will be particularly significant when the distance between the donor and the acceptor is such that there may be significant overlap between their molecular orbitals (an approximate formulation for this was developed by Dexter¹⁷). The above description also ignores the effects of relaxation in the vibrational manifold of the initial donor state.

If a distance, \mathbf{R}_{DA} , may be identified between the donor and the acceptor, and if $\mathbf{r}_D(j)$ and $\mathbf{r}_A(k)$ are the coordinates of the j th electron of the donor and k th electron of the acceptor molecules respectively, the electrostatic Coulombic interaction is given by,

$$H^{\text{Coul}} = V(\mathbf{R}_{\text{DA}}) = \frac{e^2}{2} \sum_{j,k} \frac{1}{|\mathbf{R}_{\text{DA}} + \mathbf{r}_D(j) - \mathbf{r}_A(k)|}, \quad (15)$$

and therefore,

$$\hat{H}'_{D_g A^e, D^e A_g} = \left\langle \mathbf{f}_{D_g A^e} \left| \frac{e^2}{2} \sum_{j,k} \frac{1}{|\mathbf{R}_{\text{DA}} + \mathbf{r}_D(j) - \mathbf{r}_A(k)|} \right| \mathbf{f}_{D^e A_g} \right\rangle. \quad (16)$$

Here we have introduced $\langle \mathbf{f}_{D_g A^e} |$ and $\langle \mathbf{f}_{D^e A_g} |$ as the state vectors representing the electronic state vectors for the initial and final configurations.

In Förster's theory, a further approximation is made of weak Coulombic coupling between the donor and the acceptor and $V(\mathbf{R}_{\text{DA}})$ is expanded in a multipole expansion, retaining only terms up to second order in $|\frac{\mathbf{r}_D(j) - \mathbf{r}_A(k)}{\mathbf{R}_{\text{DA}}}|$, giving

$$\hat{H}'_{D_g A^e, D^e A_g} = \frac{\mathbf{k}_{\text{DA}} |\hat{\mathbf{i}}_D \cdot \hat{\mathbf{i}}_A|}{e |\mathbf{R}_{\text{DA}}|^3}. \quad (17)$$

In deriving eq. (14), we have decoupled the electronic state vectors $\langle \mathbf{f}_{D_g A^e} |$ and $\langle \mathbf{f}_{D^e A_g} |$ into products of separate electronic states for the donor, $\langle \mathbf{f}_{D_g} |$, $\langle \mathbf{f}_{D^e} |$ and the acceptor $\langle \mathbf{f}_{A_g} |$ and $\langle \mathbf{f}_{A^e} |$, namely

$$\langle \mathbf{f}_{D_g A^e} | = \langle \mathbf{f}_{D_g} | \langle \mathbf{f}_{A^e} | \quad \text{and} \quad \langle \mathbf{f}_{D^e A_g} | = \langle \mathbf{f}_{D^e} | \langle \mathbf{f}_{A_g} |, \quad (18)$$

such that

$$\mathbf{i}_{D(A)} = \langle \mathbf{f}_{D^e(A^e)} | e \sum_j \mathbf{r}_{D(A)}(j) | \mathbf{f}_{D_g(A_g)} \rangle, \quad (19)$$

is the dipole moment of a point dipole located on the donor (acceptor). The factor \mathbf{k}_{DA} is an orientational factor related to relative orientation of the donor and the acceptor.

Conventionally, the emission spectrum of the donor, $I_D(\mathbf{w})$ and the absorption coefficient of the acceptor, $\mathbf{a}_A(\mathbf{w})$ are defined in the context of radiative processes as follows:

$$\mathbf{a}_A(\mathbf{w}) = C_A |\mathbf{i}_A|^2 \sum_{v_{A_g}} \sum_{v_{A^e}} f_{v_{A_g}} |\langle \mathbf{c}_{v_{A_g}} | \mathbf{c}_{v_{A^e}} \rangle|^2 \mathbf{d}(E - E_{A^e, v_{A^e}} + E_{A_g, v_{A_g}}), \quad (20)$$

$$I_D(\mathbf{w}) = \frac{C_D \mathbf{w}^3}{k_{\text{rad}}} |\mathbf{i}_D|^2 \sum_{v_{D^e}} \sum_{v_{D_g}} f_{v_{D^e}} |\langle \mathbf{c}_{v_{D_g}} | \mathbf{c}_{v_{D^e}} \rangle|^2 \mathbf{d}(E_{D^e, v_{D^e}} - E_{D_g, v_{D_g}} - E), \quad (21)$$

where Franck–Condon factors for the donor de-excitation, $|\langle \mathbf{c}_{D_g} | \mathbf{c}_{D^e} \rangle|^2$ and acceptor excitation, $|\langle \mathbf{c}_{A_g} | \mathbf{c}_{A^e} \rangle|^2$ appear separately in eqs (20) and (21) respectively, the functions \mathbf{c}_i being the vibrational wavefunctions for the species i . The energy $E = \hbar\mathbf{w}$, is the amount transferred in the resonant exchange. The delta functions meet the resonance conditions for the corresponding radiative processes. The constants C_A and C_D are related to the refractive index, velocity of light and dielectric constant of the medium; k_{rad} is the radiative rate constant. The connection with eq. (13) can now be established keeping in mind the following definitions,

$$A_A(t) = \frac{3\hbar nc}{4\mathbf{p}^2} \int_{-\infty}^{\infty} \frac{d\mathbf{w}}{\mathbf{w}} e^{i\mathbf{w}t} \mathbf{a}_A(\mathbf{w}), \quad (22)$$

where n is the refractive index and c the velocity of light,

$$f_D(t) = 2\mathbf{p} \sum_{v_{D_g}} \sum_{v_{D^e}} f_{v_{D^e}} |\langle \mathbf{c}_{v_{D_g}} | \mathbf{c}_{v_{D^e}} \rangle|^2 e^{\frac{i}{\hbar}(E_{D^e, v_{D^e}} - E_{D_g, v_{D_g}})t}, \quad (23)$$

$$\mathbf{d}(\mathbf{w}) = \frac{1}{2\mathbf{p}} \int_{-\infty}^{\infty} e^{i\mathbf{w}t} dt, \quad (24)$$

and finally,

$$\begin{aligned} & \mathbf{d}(E_{D^e, v_{D^e}} + E_{A_g, v_{A_g}} - E_{D_g, v_{D_g}} - E_{A^e, v_{A^e}}) \\ &= \int dE \mathbf{d}(E_{D^e, v_{D^e}} - E_{D_g, v_{D_g}} - E) \mathbf{d}(E - E_{A^e, v_{A^e}} + E_{A_g, v_{A_g}}). \end{aligned} \quad (25)$$

Thus we get,

$$k_{DA}^{\text{Förster}} = \frac{\text{Constant}}{R^6} \times k_{\text{rad}} \int_0^{\mathbf{w}} \frac{d\mathbf{w}}{\mathbf{w}^4} I_D(\mathbf{w}) \mathbf{a}_A(\mathbf{w}) = k_{\text{rad}} \left(\frac{R_F}{R} \right)^6, \quad (26)$$

where $R = \mathbf{R}_{DA}$ and R_F called Förster radius is defined as the DA separation at which the transfer rate is equal to the radiative decay rate of the donor.

$$R_F^6 = \frac{9c^4 \mathbf{k}_{DA}^2}{8\mathbf{p}e^2 n^4} \int_0^{\mathbf{w}} \frac{d\mathbf{w}}{\mathbf{w}^4} I_D(\mathbf{w}) \mathbf{a}_A(\mathbf{w}). \quad (27)$$

Equations (26) and (27) together are the more commonly expressed phenomenological versions of Förster EET rate expression. It should be clear from the above that assumptions of (i) equilibrated initial excited donor and ground acceptor states, (ii) Coulombic interaction between the donor and the acceptor, (iii) weak Coulombic coupling, i.e. point dipole–point dipole interaction and (iv) complete separation of the donor and acceptor energy states as well as a separation of the electronic and vibrational motions of each, are necessary to derive the Förster expression. In spite of these assumptions, Förster expression has worked reasonably well for reasonably large distances, $O(\geq 100)\text{\AA}$, between the donor and the acceptor.

Distance dependence of Coulombic energy transfer rate

In order to explore the validity of the Förster expression for distance dependence, we have carried out a quantum chemical calculation of the rate between polyfluorene (PF₆) and triphenyl (TPP)¹⁸. Here PF₆ is the donor and

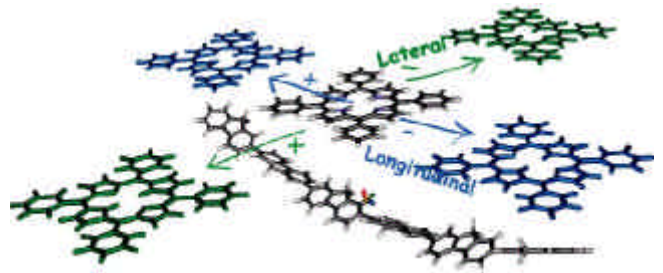


Figure 3. Geometrical arrangement of PF₆ and TPP for study of excitation transfer rates associated with longitudinal or lateral displacement of the acceptor. Reference position of TPP corresponds to cofacial parallel or cofacial orthogonal orientation at a DA separation of 10 Å and the red green blue (RGB) axes define the reference frame of each molecule where the B-axis (z-axis) shows the transition dipole moment vector direction. Displacement of TPP along the z-axis is defined as the longitudinal direction, while displacement perpendicular to the transition dipole vector in the plane of the TPP molecule (along the x-axis) is defined as the lateral direction. Arbitrary choice of positive (+) and negative (–) displacement directions is also defined.

TPP is the acceptor. In Figure 3 we show the geometry of the donor and acceptor and also the manner in which separation between them is varied. The calculation of the rate has been carried out using the Fermi Golden Rule. We compute the full resonance-Coulomb coupling matrix element as well as the point-dipole approximation.

Classic semi-empirical Pariser–Parr–Pople (PPP) Hamiltonian, coupled with single configuration interaction (SCI) was used to carry out the necessary calculations. From the PPP/SCI wave functions, electronic transition energies and transition dipole moments were calculated based on optimized geometries.

In Figure 4, we show the calculated distance dependence for a given transition. We also show comparison with the point-dipole approximation, calculated within the same wave functions. Figure 4 shows that the rate deviates from $1/R^6$ distance dependence at small separation.

Several comments on the above result are in order. Point-dipole approximation and Förster expression should remain valid when the distance is large compared to the size of the donor–acceptor system. Therefore, in those applications of FRET where donor and acceptor are dye molecules of molecular dimension, say L , Förster expression is expected to remain valid till R is larger than or comparable to L .

Energy transfer between a dye and a nanoparticle

The ruler-like feature of FRET has found remarkable application in the EET between a dye and a nanoparticle separated by a suitable spacer². An interesting example of this is when the spacer is a DNA⁸. The breakdown of Förster expression is widely observed in such systems and a vari-

able profile for the quantum efficiency as a function of the distance between the donor and the acceptor is seen as shown below,

$$k_{DA}^{\text{Förster}} = k_{\text{rad}} \left(\frac{R_0}{R} \right)^n \quad (28)$$

The index n has the value 6 for the classic Förster case with $R_0 = R_F$ and is generally less than 6 for dye–nanoparticle systems. In a recent example of a fluorescein–DNA spacer–gold nanoparticle system, the value of n was found to be 4 for a large range of values of R^4 .

Attempts have been made to explain this deviation by invoking a surface excitation transfer^{18,20} involving excitation of states below the Fermi level of a metal surface as the absorbing entities. The value of the index n is then 4 even for very large values of R . However, this is strictly valid for metal surfaces only and a more specific treatment of the nanosystem is desirable.

The problem in case of the nanoparticle is that it is neither so small such that the derivation for EET rate described earlier for a single absorber molecule is valid, nor is it large enough such that the solid state theory of metallic crystals can be fully invoked. A meaningful way of modelling such a system would be to consider a distribution of electric charge for the electrons in the acceptor in terms of a charge density on the nanosystem. The assumption of Coulombic coupling may still be retained. Further, let us assume that the donor dye molecule interacts with the acceptor via a point dipole located suitably, for instance, at the centre of gravity. Thus eq. (15) is replaced by

$$H^{\text{Coul}} = V(\mathbf{R}_{DA}) = \int_V d\mathbf{r}' \frac{\hat{\mathbf{r}}_{D'} \cdot (\hat{\mathbf{R}}_{DA} - \mathbf{r}')}{|\mathbf{R}_{DA} - \mathbf{r}'|^2} \mathbf{r}(\mathbf{r}'), \quad (29)$$

where V is the physical space occupied by the nanoparticle, $\hat{\mathbf{r}}_{D'}$ is the dipole operator for the donor, $\mathbf{r}(\mathbf{r}')$ is the charge density distribution in the nanoparticle, \mathbf{r}' being a

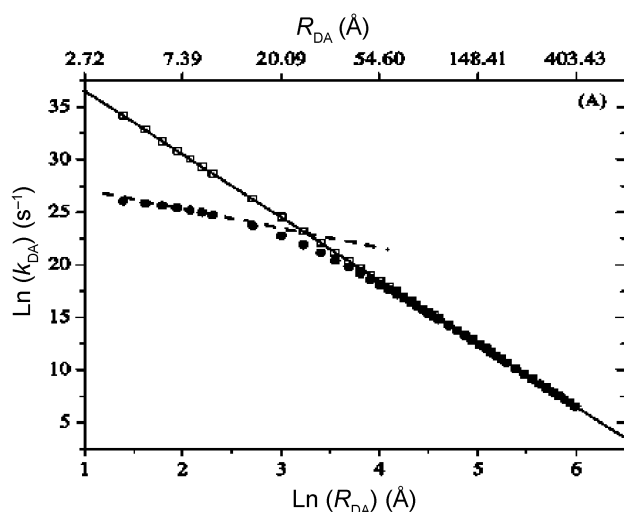


Figure 4. Distance dependence of rate for cofacial parallel orientation of PF₆ and TPP. Open squares represent Förster rate and filled circles show the resonance-Coulomb rates calculated within the PPP/SCI framework. EET takes place between the donor molecule of wavelength 358 nm and acceptor molecule of wavelength 367 nm. The traditional R_{DA}^6 distance dependence is shown by solid line and numerical fit of the resonance-Coulomb rates to R_{DA}^{-2} by dashed line.

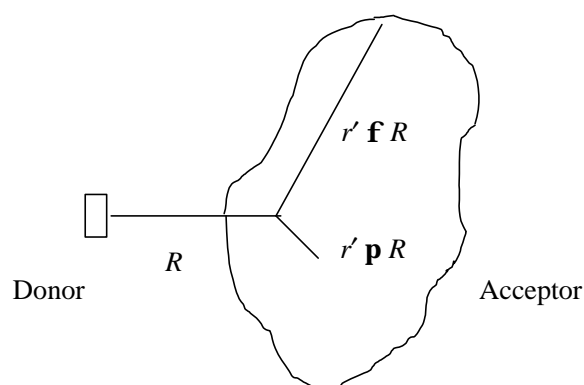


Figure 5. Schematic picture of donor–acceptor interaction, where the donor is a dye molecule and acceptor a nanoparticle.

coordinate with respect to the CM of the nanoparticle, $\hat{\mathbf{R}}_{\text{DA}}$ and $\hat{\mathbf{r}}'$ are the unit vectors in the direction of \mathbf{R}_{DA} and \mathbf{r}' respectively. In what follows, we write \mathbf{R}_{DA} as \mathbf{R} for convenience.

Similar to the discussion earlier, the integrand in eq. (2) can be expanded in a multipole expansion retaining only terms up to the first order. Thus we obtain

$$V(\mathbf{R}) = \hat{\mathbf{i}}_{\text{D}} \cdot \int_V d\mathbf{r}' (\hat{\mathbf{R}} - \hat{\mathbf{r}}') \left[\frac{1}{R} + \frac{\mathbf{R} \cdot \hat{\mathbf{r}}'}{R^2} + Q \right] \mathbf{r}(\mathbf{r}') \quad (30)$$

where $\mathbf{r}_{f(\mathbf{p})}$ is a vector with magnitude $r_{f(\mathbf{p})}$ equal to greater (lesser) of $R = |\mathbf{R}|$ and $r' = |\mathbf{r}'|$, Q refers to terms of quadrupolar and higher order. For $r_f = R$, this becomes

$$V(\mathbf{R}) = \hat{\mathbf{i}}_{\text{D}} \cdot \left[\int_{r' \mathbf{p} R} d\mathbf{r}' (\hat{\mathbf{R}} - \hat{\mathbf{r}}') \left(\frac{1}{R} + \frac{\mathbf{r}' \cdot \hat{\mathbf{R}}}{R^2} + Q \right) \mathbf{r}(\mathbf{r}') + \int_{r' \mathbf{f} R} d\mathbf{r}' (\hat{\mathbf{R}} - \hat{\mathbf{r}}') \left(\frac{1}{r'} + \frac{\mathbf{R} \cdot \hat{\mathbf{r}}'}{r'^2} + Q \right) \mathbf{r}(\mathbf{r}') \right] \quad (31)$$

To achieve the EET rate as from eq. (14), we need to evaluate V_{DA} , i.e. $\langle D^e A_g | V(\mathbf{R}) | D_g A^e \rangle$. A decoupling approximation is made here as follows:

$$V_{\text{DA}} = \langle \mathbf{f}_{D^e} \mathbf{f}_{A_g} | V(\mathbf{R}) | \mathbf{f}_{D_g} \mathbf{f}_{A^e} \rangle. \quad (32)$$

Also, charge density may be written as a sum over contributions from individual electronic charges,

$$\int d\mathbf{r}' f(\mathbf{r}') \mathbf{r}(\mathbf{r}') = \sum_i \mathbf{r}_i(\mathbf{r}') f(\mathbf{r}'), \quad (33)$$

where $\mathbf{r}_i(\mathbf{r}')$ is the contribution to the total charge density from the i th electron in the nanoparticle and $f(\mathbf{r}')$ is a continuous function of \mathbf{r}' . This gives,

$$V_{\text{DA}} = \hat{\mathbf{i}}_{\text{D}} \cdot \sum_i \left[\left\langle \mathbf{f}_{A_g} \left| \left(\hat{\mathbf{R}} - \hat{\mathbf{r}}' \right) \left(\frac{1}{R} + \frac{\mathbf{r}' \cdot \hat{\mathbf{R}}}{R^2} + Q \right) \mathbf{r}_i(\mathbf{r}') \right| \mathbf{f}_{A^e} \right\rangle_{r' \mathbf{p} R} + \left\langle \mathbf{f}_{A_g} \left| \left(\frac{1}{r'} + \frac{\mathbf{R} \cdot \hat{\mathbf{r}}'}{r'^2} + Q \right) \mathbf{r}_i(\mathbf{r}') \right| \mathbf{f}_{A^e} \right\rangle_{r' \mathbf{f} R} \right], \quad (34)$$

where

$$\mathbf{m}_{\mathbf{b}} = \langle \mathbf{f}_{D^e} | \hat{\mathbf{m}} | \mathbf{f}_{D_g} \rangle, \quad (35)$$

and the matrix elements are now evaluated by integration over only the part of the configuration space specified by the subscripts $R \mathbf{f} r'$ (first term) and $R \mathbf{p} r'$ (second term). It can be seen easily that the lowest order term is

$$V_{\text{DA}}^{(1)} = \hat{\mathbf{i}}_{\text{D}} \cdot \sum_i \left[\frac{1}{R^2} \left\langle \mathbf{f}_{A_g} \left| \left(\hat{\mathbf{R}} - \hat{\mathbf{r}}' \right) \mathbf{r}_i(\mathbf{r}') \right| \mathbf{f}_{A^e} \right\rangle_{r' \mathbf{p} R} + \left\langle \mathbf{f}_{A_g} \left| \left(\hat{\mathbf{R}} - \hat{\mathbf{r}}' \right) \frac{\mathbf{r}_i(\mathbf{r}')}{r'^2} \right| \mathbf{f}_{A^e} \right\rangle_{r' \mathbf{f} R} \right], \quad (36)$$

Typically, for a metallic nanoparticle like a cluster of gold atoms, $\langle \mathbf{f}_{A_g} |$ and $\langle \mathbf{f}_{A^e} |$ are excitonic states undergoing plasmonic excitations. The corresponding wavefunctions are delocalized functions spread all over the nanoparticle, with the extent of delocalization dependent on the size of the system. When R is reasonably small (not too small so that the direct overlap of orbitals between the donor and acceptor becomes significant) and the nanoparticle is fairly large, contribution of the second term will be relatively large. It can be seen more clearly by writing the radial and polar integration variables separately.

$$V_{\text{DA}}^{(1)} = \hat{\mathbf{i}}_{\text{D}} \cdot \sum_i \int d\Omega' \left[\frac{1}{R^2} \int_{r' \mathbf{p} R} d\mathbf{r}' r'^2 \mathbf{f}_{A_g}^*(r') (\hat{\mathbf{R}} - \hat{\mathbf{r}}') \mathbf{r}_i(\mathbf{r}') \mathbf{f}_{A^e}(r') + \int_{r' \mathbf{f} R} d\mathbf{r}' \mathbf{f}_{A_g}^*(r') (\hat{\mathbf{R}} - \hat{\mathbf{r}}') \mathbf{r}_i(\mathbf{r}') \mathbf{f}_{A^e}(r') \right], \quad (37)$$

where Ω' is the variable for integration over the spherical polar space.

The two terms in eq. (37) differ from each other by (i) presence of the factor $(r^2/R^2) \in (0, 1)$ in the first term and (ii) for large nanoparticle sizes, the second term has a much larger volume of integration also. In such a case, the variation of $V_{\text{DA}}^{(1)}$ with R will be quite complex and less attenuated than R^{-2} and hence from eq. (14), that of the EET rate with R will be less attenuated than R^{-4} . In particular, if in the core regions of the nanoparticle, the charge density is approximated by an average value \bar{r} for the first term in eq. (37), say $V_{\text{DA}_1}^{(1)}$, we get

$$V_{\text{DA}_1}^{(1)} = \hat{\mathbf{i}}_{\text{D}} \cdot \frac{\bar{r}}{R^2} \langle \mathbf{f}_{A_g}^* | (\hat{\mathbf{R}} - \hat{\mathbf{r}}') | \mathbf{f}_{A^e} \rangle_{r' \mathbf{p} R} = \hat{\mathbf{i}}_{\text{D}} \cdot \frac{\bar{r}}{R^2} \left[\hat{\mathbf{R}} \langle \mathbf{f}_{A_g}^* | \mathbf{f}_{A^e} \rangle_{r' \mathbf{p} R} - \langle \mathbf{f}_{A_g}^* | \hat{\mathbf{r}}' | \mathbf{f}_{A^e} \rangle_{r' \mathbf{p} R} \right], \quad (38)$$

Since the state vectors $\langle \mathbf{f}_{A_g} |$ and $\langle \mathbf{f}_{A^e} |$ are orthonormal, it is likely that both the integrals in eq. (38) will have negligible values compared to the second R -independent term in eq. (36).

The familiar Förster variation of EET rate as R^{-6} is retrieved from the next higher order terms,

$$V_{\text{DA}}^{(2)} = 2\hat{\mathbf{i}}_{\text{D}} \cdot \sum_i \left[\frac{1}{R^3} \langle \mathbf{f}_{A_g} | (\hat{\mathbf{R}} - \hat{\mathbf{r}}') \mathbf{r}' \hat{\mathbf{R}} \mathbf{r}_i(\mathbf{r}') | \mathbf{f}_{A^e} \rangle_{r' \mathbf{p}R} + \langle \mathbf{f}_{A_g} | (\hat{\mathbf{R}} - \hat{\mathbf{r}}') \mathbf{R} \hat{\mathbf{r}}' \frac{\mathbf{r}_i(\mathbf{r}')}{r'^3} | \mathbf{f}_{A^e} \rangle_{r' \mathbf{f}R} \right]. \quad (39)$$

When R is very large compared to the size of the nanoparticle, the Coulombic interaction is effectively between two transition dipoles with a variation as R^{-3} and Förster rate as R^{-6} .

We have thus demonstrated qualitatively by considering the size of the acceptor comparable to or larger than the distance of separation between the donor and the acceptor that in such cases, one may expect much weaker distance (even as weak as $1/R^2$) dependence than the Förster rate expression. This is observed in FRET experiments widely. Thus the problem left to be solved is to find a phenomenological/spectroscopic means analogous to eq. (26) for the dye–nanoparticle system, i.e. whether an expression like eq. (28) could be written where $R_0 = R_F$ is defined in terms of spectral overlap between donor fluorescence and acceptor absorbance characteristics.

We can write in general,

$$|V_{\text{DA}}|^2 = |\hat{\mathbf{i}}_{\text{D}}|^2 \left(a + \frac{b}{R^2} + \dots \right), \quad (40)$$

where a is a quantity dimensionally similar to the square of a transition matrix element of an inverse length square over the excitonic states of the acceptor nanoparticle, while b is likewise similar to a transition dipole moment. Comparing with the derivation earlier, we can write, to the lowest order in $1/R$,

$$k_{\text{DA}} = \text{Constant} \times k_{\text{rad}} \int_0^w \frac{d\mathbf{w}}{w^4} I_D(\mathbf{w}) X_A(\mathbf{w}) = k_{\text{rad}} R_0, \quad (41)$$

where

$$X_A(\mathbf{w}) = C_A |\boldsymbol{\epsilon}_A|^2 \sum_{v_{A_g}} \sum_{v_{A^e}} f_{v_{A_g}} |\langle \mathbf{c}_{v_{A_g}} | \mathbf{c}_{v_{A^e}} \rangle|^2 \mathbf{d}(E - E_{A^e, v_{A^e}} + E_{A_g, v_{A_g}}), \quad (42)$$

and

$$\boldsymbol{\epsilon}_A \approx \sum_i \left\langle \mathbf{f}_{A_g} \left| (\hat{\mathbf{R}} - \hat{\mathbf{r}}') \frac{\mathbf{r}_i(\mathbf{r}')}{r'^2} \right| \mathbf{f}_{A^e} \right\rangle_{r' \mathbf{f}R}, \quad (43)$$

all terms being as described earlier. Thus we have retrieved a description similar to the one presented earlier, except that the absorption coefficient $\mathbf{s}_A(\mathbf{w})$ is replaced by the quantity $X_A(\mathbf{w})$ and

$$R_0 = \frac{9c^4}{8\pi e^2 n^4} \int_0^w \frac{d\mathbf{w}}{w^4} I_D(\mathbf{w}) X_A(\mathbf{w}). \quad (44)$$

The analysis may be extended further to the terms containing higher powers of $1/R$ in eq. (40).

A summary of the theoretical results discussed above is as follows: The rate profile of EET with respect to the distance between the donor and the acceptor may be classified in three different regimes. When the distance R_{DA} is too small, overlap between the orbitals of the donor and acceptor molecules makes it difficult to define a clear profile. In this regime, Dexter mechanism resulting in exponential variation of rate with R may dominate. When the distance is very large ($O(\geq 100)\text{\AA}$) and the Coulombic coupling between the donor and acceptor can be approximated by the dipole–dipole interaction term, then the classic Förster variation as R^{-6} is seen. In the regime of intermediate distances between the donor and the acceptor, the profile may go as R^{-4} , or as R^{-2} , or it may even be independent of R , depending on how small R is and the nature of the systems involved. If either the donor or the system is large with an average radius comparable to or larger than the donor–acceptor separation, it is necessary to go beyond a dipole–dipole interaction and consider interaction between a charge density distribution on it interacting with a transition dipole or a similar charge density distribution on the other species. Such a treatment of the problem provided us with a rate profile that depends on anywhere between zeroth to fourth inverse power of donor–acceptor separation, depending on relatively how large the donor or acceptor entity is. We have also surmised that a quantity akin to the Förster radius R_F related to spectroscopic parameters may be described for these intermediate regimes also.

FRET and polymer dynamics

As discussed elaborately in the previous sections, FRET is the transfer of the excited state energy from an excited donor to an acceptor. This transfer occurs without the appearance of a photon and results primarily due to the Coulombic interaction between a donor and acceptor. Recently, FRET has emerged as a powerful technique to study both the conformation and dynamics of polymers and bio-polymers. One can combine FRET with single-molecule spectroscopic techniques to obtain histograms of energy transfer efficiency which provides valuable information about the temperature and denaturant-dependent conformational states of the protein²¹. We now discuss means to deal with the fluctuation in distance between the donor and acceptor species and also aspects of FRET efficiency.

Wilemski–Fixman theory

In 1974, Wilemski and Fixman²² (WF) presented an elegant theory for diffusion limited intrachain reaction of a flexible polymer chain. WF considered a simple Rouse model²³ to describe the polymer chain with N monomers. In Rouse chain, the hydrodynamic and excluded volume interactions are absent.

FRET in disordered systems presents a complex problem²⁴. The complexity of describing the dynamics of energy transfer of polymers in solution arises from the fact that due to chain connectivity, the Brownian motion of monomers on the polymer is strongly correlated. The many-body nature of the polymer dynamics can be described by a joint, time-dependent probability distribution $P(\mathbf{r}^N, t)$ where \mathbf{r}^N denotes the position of all the N polymer beads at time t . The time dependence of the probability distribution $P(\mathbf{r}^N, t)$ can be described by reaction-diffusion equation²² as given below:

$$\frac{\partial}{\partial t} P(\mathbf{r}^N, t) = L_B P(\mathbf{r}^N, t) - k_0 S(R) P(\mathbf{r}^N, t), \quad (45)$$

where $k_0 S(R)$ is the sink term and L_B is the full $3N$ dimensional diffusion tensor given as,

$$L_B(\mathbf{r}, t) = D \sum_{j=1}^N \frac{\partial}{\partial r_j} P_{\text{eq}}(\mathbf{r}, t) \frac{\partial}{\partial r_j} \frac{P(\mathbf{r}, t)}{P_{\text{eq}}(\mathbf{r}, t)}, \quad (46)$$

where the subscript 'eq' denotes equilibrium, R is the scalar distance between the two ends of the polymer chain and D is defined as the centre of mass diffusion coefficient.

The survival probability, $S_p(t)$ is defined as the probability that the chain has not reacted after time t and is given by,

$$S_p(t) = \int P(\mathbf{r}^N, t) dr_1 dr_2 \dots dr_N. \quad (47)$$

The Laplace transform of the survival probability is

$$\hat{S}_p(s) = \frac{1}{s} - \frac{k v_{\text{eq}}}{s^2 (1 + k \hat{D}(s) / v_{\text{eq}})}, \quad (48)$$

where s is the Laplace variable, $D(t)$ is the Green's function and v_{eq} is the equilibrium rate.

WF theory was applied to Rouse chain with Heaviside sink function. This theory provides the understanding of time-dependent energy transfer processes because time-resolved FRET experiments can be an important tool in understanding the folding/unfolding transitions. Lakshminanth *et al.*²⁵ performed time-resolved fluorescence with the maximum entropy method to analyse the decay kinetics, on a small protein barstar to show the existence of many equilibrium unfolding states contrary to the belief of the two state model of protein folding. WF theory with suitable modification can be used to understand protein folding²⁶.

FRET efficiency

FRET can serve as a probe to study the structural morphology of a polymer chain. Recently, computational studies of

Förster energy transfer efficiency^{7,8,21} showed that it can indeed differentiate between different conformational states of collapsed polymer, such as rods, toroids or simply the collapsed disordered state. Experimental studies^{7,21} demonstrated that the single molecular spectroscopy can be used to obtain FRET efficiency distribution. FRET efficiency distribution (Φ_F) is defined by the following relation:

$$\Phi_F = \frac{k(R)}{k(R) + k_{\text{rad}}}, \quad (49)$$

where R is the distance between the donor and acceptor. Assuming the reaction rate to be given by the Förster rate from eq. (1), we get

$$\Phi_F = \frac{1}{1 + (R/R_F)^6}. \quad (50)$$

The probability of FRET efficiency distribution $P(\Phi_F)$ can be defined by the following expression,

$$P(\Phi_F) = \frac{1}{N} \sum_{i=1}^N d(\Phi_F - \Phi_F(\mathbf{t}_{\text{rad}})). \quad (51)$$

In each simulation, after choosing a donor-acceptor pair at time $t = 0$, the pair is followed till the trajectory gets terminated due to energy transfer between the donor and acceptor pair. Here, N is the total number of independent polymer chains, and t_{rad} is the time taken for a trajectory to terminate from the time of its generation.

Comparison between WF theory and simulation

The predictions of WF theory are compared with Brownian dynamics (BD) simulations on Rouse chain model²³. Rouse chain is a simple polymer model having only bonding interaction and no excluded volume. This is called the ideal chain. BD simulations are carried out for an ideal Rouse chain, where the neighbouring beads interact via a harmonic potential U given by,

$$bU = \frac{3}{2b^2} \sum_{j=1}^N (r_j - r_{j+1})^2, \quad (52)$$

where b^{-1} is the Boltzmann constant times the temperature, r_j is the position vector of bead j , and the number of beads constituting the polymer chain is $N + 1$. The mean square bond length is b^2 . The equation of motion of the beads under Brownian motion is given by,

$$r_j(t + \Delta t) = r_j(t) + F_j(t)\Delta t + \Delta X^G(t), \quad (53)$$

where $r_j(t)$ is the position of j th particle at time t , $F_j(t)$ is the systematic force and $\Delta X^G(t)$ is the random force ob-

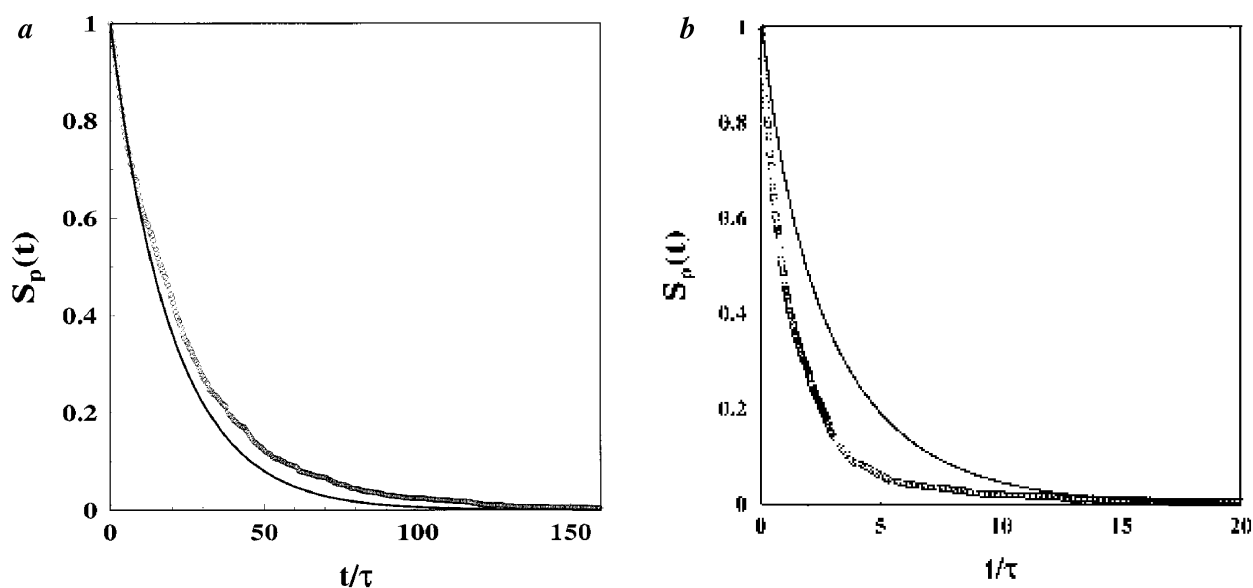


Figure 6. Comparison of simulation results (symbols) for $S_p(t)$ to predictions of the WF theory (line) for (a) a large Förster rate, namely $k_F = 10$ at $R_F = 1$ for $N = 50$, and (b) for a longer chain ($N = 100$) at $R_F = 8$ and $k_F = 1$.

tained from a Gaussian distribution with zero mean and standard deviation of $2D\Delta t$. In eq. (53) the time and energy scales are fixed using units where $\mathbf{b} = 1$, the bead diffusion coefficient $D_0 = 1$, and the mass of bead $m = 1$. All the results are presented in these dimensionless units. Δt is varied between 0.0001 and 0.01, depending on the R_F value. Larger the R_F , greater is the requirement for the smaller time step. For example, at $k_F = 1$, when $R_F = 1$, a value of $\Delta t = 0.01$ is used and for $R_F = 5$, a much smaller time step, $\Delta t = 0.0002$ is used.

Survival probabilities obtained from BD simulations agree well with predictions of WF theory. Although the agreement is good for small R_F values, simulation results start deviating from WF at larger R_F values^{27–29}. Here comparison between simulation results and WF theory is shown for different Förster rates k_F . Figure 6a shows results for large Förster rate, while Figure 6b shows results for small Förster rate, but relatively larger Förster radius. The decay of survival probability is generally non-exponential, more so when the Förster radius is less than the radius of the polymer. The WF theory requires modification when Förster rate is much faster than the rate of diffusion. Such a modification has recently been carried out³⁰.

Conclusion

The pivotal role of FRET in the fast developing area of biodynamics is well established. Most FRET studies investigate Förster-type energy transfer pathways, with the rate of EET varying with the distance between the donor and acceptor, R , as R^{-6} . However, it is found in numerous experiments that when the donor–acceptor separation is comparable to the size of the donor and/or acceptor molecule,

i.e. R is not large enough, the rate profile is less attenuated and can be as weak as R^{-2} , more commonly⁷ R^{-4} . Here we have critically examined the limitations in Förster theory and underlined the questionable assumptions ranging from that of equilibrium prior to the EET process – thus ignoring the role of the vibrational manifold in the fast processes taking place to the weak Coulombic coupling between point dipoles located on the donor and acceptor, which is not valid for donor/acceptor sizes comparable to the separation distance. We have attempted a modified theoretical formulation of the problem, specifically for the application to dye–nanoparticle system, and have shown that the lowest order term in the rate profile is independent of R . It is desirable that a final expression similar to Förster expression relating the rate of EET to line shape function of the emission spectrum of the donor and absorption coefficient of the acceptor be obtained. Numerical simulations for the case of a segment of a conjugated polymer (PF₆) as a donor and TPP as an acceptor using the semi-empirical quantum chemical methods were discussed. Fluctuations in the magnitude of R were dealt with using BD simulations within WF theory on a Rouse model.

The results and arguments presented here and elsewhere¹⁶ clearly indicate the need to go beyond Förster approach and WF theory for understanding FRET results. With the explosion in the studies on nano–bio systems and the increasing amounts of information about such systems becoming accessible, alternatives to Förster EET rate theory and WF theory of diffusion on flexible polymer chains will draw increasing attention³¹.

1. Lakowicz, J. R., In *Principles of Fluorescence Spectroscopy*, Plenum, New York, 1983; Scholes, G. D., Long-range resonance energy

- transfer in molecular systems. *Annu. Rev. Phys. Chem.*, 2003, **54**, 57–87; May, V. and Kuhn, O., In *Charge and Energy Transfer Dynamics in Molecular Systems*, Wiley-VCH, Verlag, Berlin, 2000.
2. Förster, Th., Delocalized excitation and excitation transfer. In *Modern Quantum Chemistry, Istanbul Lectures, Part III: Action of Light and Organic Crystals* (ed. Sinanoglu, O.), Academic Press, New York, 1965, p. 93.
 3. Schuler, B., Lipman, E. A., Steinbach, P. J., Kumke, M. and Eaton, W. A., Polyproline and the 'spectroscopic ruler' revisited with single molecule fluorescence. *Proc. Natl. Acad. Sci. USA*, 2005, **102**, 2754–2759.
 4. Herz, L. M., Silva, C., Grimsdale, A. C., Müllen, K. and Phillips, R. T., Time-dependent energy transfer rates in a conjugated polymer guest–host system. *Phys. Rev. B*, 2004, **70**, Art. No. 165207; Hennebicq, E. *et al.*, Exciton migration in rigid-rod conjugated polymers: An improved Förster model. *J. Am. Chem. Soc.*, 2005, **127**, 4744–4762.
 5. Cerullo, G., Stagira, G., Zavelani-Rossi, M., De Silvestri, S., Virgili, T., Lidzey, D. G. and Bradley, D. D. C., Ultrafast Förster transfer dynamics in tetraphenylporphyrin doped poly(9,9-dioctyl fluorene). *Chem. Phys. Lett.*, 2001, **335**, 27–29.
 6. Hu, D., Yu, J. and Barbara, P. F., Single-molecule spectroscopy of the conjugated polymer MEH–PPV. *J. Am. Chem. Soc.*, 1999, **121**, 6936–6937.
 7. Deniz, A. A. *et al.*, Single-molecule protein folding: Diffusion fluorescence resonance energy transfer studies of the denaturation of chymotrypsin inhibitor 2. *Proc. Natl. Acad. Sci. USA*, 2000, **97**, 5179–5184.
 8. Weiss, S., Measuring conformational dynamics of biomolecules by single molecule fluorescence spectroscopy. *Nature Struct. Biol.*, 2000, **7**, 724–729.
 9. Yun, C. S. *et al.*, Nanometal surface energy transfer in optical rulers. Breaking the FRET barrier. *J. Am. Chem. Soc.*, 2005, **127**, 3115–3119.
 10. Hofkens, J. *et al.*, Revealing competitive Förster-type resonance energy-transfer pathways in single bichromophoric molecules. *Proc. Natl. Acad. Sci. USA*, 2003, **100**, 13146–13151.
 11. Birch, D. J. S., Holmes, A. S. and Darbyshire, M., Intelligent sensor for metal ions based on fluorescence resonance energy transfer. *Meas. Sci. Technol.*, 1995, **6**, 243–247.
 12. Snyder, A. P., Sudnick, D. R., Arkle, V. K. and Horrocks, Jr. W. D., Lanthanide ion luminescence probes, Characterization of metal ion binding sites and intermetal energy transfer distance measurements in calcium-binding proteins. 2. Thermolysin. *Biochemistry*, 1981, **20**, 3334–3339.
 13. Yang, M. and Fleming, G. R., Influence of phonons on exciton transfer dynamics: comparison of the Redfield, Förster, and modified Redfield equations. *Chem. Phys.*, 2002, **282**, 163–180; Barkai, E., Jung, Y. and Silbey, R., Theory of single-molecule spectroscopy: Beyond the ensemble average. *Annu. Rev. Phys. Chem.*, 2004, **55**, 457–507.
 14. Kleima, F. J., Hoffman, E., Gobets, B., van Stokkum, I., van Grondelle, R., Diederichs, K. and van Amerongen, H., Förster excitation energy transfer in peridinin-chlorophyll *a* protein. *Biophys. J.*, 2000, **78**, 344–353.
 15. Würthner, F. and Sautter, A., Energy transfer in multichromophoric self-assembled molecular squares. *Org. Biomol. Chem.*, 2003, **1**, 240–243.
 16. Lin, S. H. *et al.*, Ultrafast dynamics and spectroscopy of bacterial photosynthetic reaction centers. *Adv. Chem. Phys.*, 2002, **121**, 1–88.
 17. Dexter, D. L., A theory of sensitized luminescence in solids. *J. Chem. Phys.*, 1953, **21**, 836–838.
 18. Wong, K. F., Bagchi, B. and Rossky, P. J., Distance and orientation dependence of excitation transfer rates in conjugated systems: Beyond the Förster theory. *J. Phys. Chem. A*, 2004, **108**, 5752–5763.
 19. Persson, B. and Lang, N., Electron–hole pair quenching of excited states near a metal. *Phys. Rev. B*, 1982, **26**, 5409–5415.
 20. Chance, R. R., Prock, A. and Silbey, R., Molecular fluorescence and energy transfer near interfaces. *Adv. Chem. Phys.*, 1978, **37**, 1–65.
 21. Deniz, A. A. *et al.*, Single-pair FRET on freely diffusing molecules: Observation of Förster distance dependence and subpopulations. *Proc. Natl. Acad. Sci. USA*, 1999, **96**, 3670–3675.
 22. Wilemski, G. and Fixman, M., Diffusion-controlled intrachain reactions of polymers. I. Theory. *J. Chem. Phys.*, 1974, **60**, 866–877; Diffusion-controlled intrachain reactions of polymers. II. Results for a pair of terminal reactive groups. *J. Chem. Phys.*, 1974, **60**, 878–890.
 23. Rouse, P. E., A theory of the linear viscoelastic properties of dilute solutions of coiling polymers. *J. Chem. Phys.*, 1953, **21**, 1272.
 24. Rolinsky, O. and Birch, D. J. S., Determination of acceptor distribution from fluorescence resonance energy transfer: Theory and simulation. *J. Chem. Phys.*, 2000, **112**, 8923–8928.
 25. Lakshmikanth, G. S., Sridevi, K., Krishnamoorthy, G. and Udgaonkar, J. B., Structure is lost incrementally during the unfolding of Barstar. *Nature Struct. Biol.*, 2001, **8**, 799.
 26. Mukherjee, A. and Bagchi, B., Correlation between rate of folding, energy landscape and topology in the folding of a model protein HP-36. *J. Chem. Phys.*, 2003, **118**, 4733; Telford, J. R., Wittung-Stafshede, P., Gray, H. B. and Winkler, J. R., Protein folding triggered by electron transfer. *Acc. Chem. Res.*, 1998, **31**, 755; Pascher, T., Chesick, J. P., Winkler, J. R. and Gray, H. B., Protein folding triggered by electron transfer. *Science*, 1996, **271**, 1558; Lyubovitsky, J. G., Gray, H. B. and Winkler, J. R., Mapping the cytochrome-*c* folding landscape. *J. Am. Chem. Soc.*, 2002, **124**, 5481; Duan, Y. and Kollman, P. A., Pathways to a protein folding intermediate observed in a 1-microsecond simulation in aqueous solution. *Science*, 1998, **282**, 740.
 27. Srinivas, G. and Bagchi, B., Detection of collapsed and ordered polymer structures by fluorescence resonance energy transfer in stiff homopolymer: Bimodality in the reaction efficiency distribution. *J. Chem. Phys.*, 2002, **116**, 837–838.
 28. Srinivas, G., Yethiraj, A. and Bagchi, B., FRET by FET and dynamics of protein folding. *J. Phys. Chem. B*, 2001, **105**, 2475.
 29. Srinivas, G. and Bagchi, B., Energy transfer efficiency distributions in polymers in solution during folding and unfolding. *Phys. Chem. Commun.*, 2002, **5**, 59.
 30. Srinivas, G., Sebastian, K. L. and Bagchi, B., Time-dependent survival probability in diffusion-controlled reaction in a polymer chain: Beyond the Wilemski–Fixman theory. *J. Chem. Phys.*, 2002, **116**, 7276–7278.
 31. Portman, J. J. and Wolynes, P. G., Complementary variational approximations for intermittency and reaction dynamics in fluctuating environments. *J. Phys. Chem. A*, 1999, **103**, 10602–10610.

ACKNOWLEDGEMENTS. H.S. thanks SSCU and IISc, for support and hospitality during his stay at Bangalore. We thank Dr G. Srinivas, IISc., Bangalore; Dr Kim Wong, Prof. Peter Rossky and Prof. Paul Barbara, UT-Austin, Texas, USA for collaboration. This work was supported in parts by grants from DST and CSIR.

Received 23 August 2005; revised accepted 21 October 2005